Docetaxel-induced apoptosis in melanoma cells is dependent on activation of caspase-2

Nizar M. Mhaidat, Yufang Wang, Kelly A. Kiejda, Xu Dong Zhang, and Peter Hersey

Immunology and Oncology Unit, Newcastle Misericordiae Hospital, Newcastle, New South Wales, Australia

Abstract

Taxanes have a broad spectrum of activity against various human cancers, including melanoma. In this study, we have examined the molecular mechanism of docetaxel-induced apoptosis of human melanoma. We report that docetaxel induced varying degrees of apoptosis in a panel of melanoma cell lines but not in normal fibroblasts. Induction of apoptosis was caspase dependent and associated with changes in mitochondrial membrane potential that could be inhibited by overexpression of Bcl-2. Docetaxel induced changes in Bax that correlated with sensitivity to docetaxel-induced apoptosis. These changes in Bax were not inhibited by overexpression of Bcl-2. Kinetic studies of caspase-2 activation by Western blotting and fluorogenic assays revealed that activation of caspase-2 seemed to be the initiating event. Inhibition of caspase-2 with z-VDVAD-fmk or by small interfering RNA knockdown inhibited changes in Bax and mitochondrial membrane potential and events downstream of mitochondria. Activation of caspase-8 and Bid seemed to be a late event, and docetaxel was able to induce apoptosis in cells deficient in caspase-8 and Bid. p53 did not seem to be involved as a p53 null cell line was sensitive to docetaxel and an inhibitor of p53 did not inhibit apoptosis. Small interfering RNA knockdown of PUMA and Noxa also did not inhibit apoptosis. These results suggest that docetaxel induces apoptosis in melanoma cells by pathways that are dependent on activation of caspase-2, which initiates mitochondrial dependent apoptosis by direct or indirect activation of Bax. [Mol Cancer Ther 2007;6(2):752–61]

Received 9/13/06; revised 11/20/06; accepted 12/20/06.

Grant support: New South Wales State Cancer Council and National Health and Medical Research Council, Australia. X.D. Zhang is a Cancer Institute NSW Fellow.

The costs of publication of this article were defrayed in part by the payment of page charges. This article must therefore be hereby marked *advertisement* in accordance with 18 U.S.C. Section 1734 solely to indicate this fact.

Requests for reprints: Peter Hersey or Xu Dong Zhang, Immunology and Oncology Unit, Royal Newcastle Hospital, Room 443, David Maddison Clinical Sciences Building, Corner King and Watt Streets, Newcastle, NSW 2300, Australia. Phone: 61-2-49-236828; Fax: 61-2-49236184. E-mail: Peter.Hersey@newcastle.edu.au or Xu.Zhang@newcastle.edu.au

doi:10.1158/1535-7163.MCT-06-0564

Introduction

The treatment of patients with metastatic melanoma continues to be a therapeutic challenge, and their prognosis is very poor. This is largely due to its unresponsiveness to conventional chemotherapeutic and biological reagents, which has been attributed to development of resistance to apoptosis (1–3). Understanding and overcoming resistance mechanism(s) of melanoma to apoptosis would therefore facilitate identification of new therapeutic targets and development of new treatments (4–6).

Taxanes, such as paclitaxel and docetaxel, represent an important class of anticancer agents that have anticancer effects *in vitro* and *in vivo* against cancers of lung, ovaries, breast, leukemia, and malignant melanoma (7). They were isolated from the bark of the American yew (*Taxus brevifolia*) and later synthesized from the foliage and seeds of European yew (*Taxus baccata*). Initially, taxanes were described as antimitotic agents that bind to β-tubulin, resulting in block of the cell cycle at the G_2-M phase and apoptosis of cells (8, 9). When given as a single agent, taxanes have produced low response rates (3.3–17%) in patients with melanoma. In some patients, taxanes were associated with prolonged duration of disease control. Higher response rates were seen (12–41%) when taxanes were given in association with other anticancer agents, such as temozolomide, dacarbazine, cisplatin, carboplatin, or tamoxifen (10, 11).

Chemotherapeutic agents in general are believed to induce apoptosis through the intrinsic mitochondrial pathway via release of apoptogenic proteins such as cytochrome *c* and second mitochondrial-derived activator of caspase/direct inhibitor of apoptosis–binding protein with low isoelectric point (Smac/DIABLO; refs. 12–16). In one model of apoptotic regulation, apoptotic stimuli such as damage to DNA or the cytoskeleton, or interaction of cells with death-inducing ligands such as tumor necrosis factor–related apoptosis–inducing ligand (TRAIL), induce activation of proapoptotic BH3-only ''sensor'' proteins of Bcl-2 family, such as Noxa, PUMA, Bim, and Bid. The sensor proteins are believed to bind to the antiapoptotic Bcl-2 family members and promote binding of the multidomain proapoptotic proteins Bax and Bak to the mitochondrial outer membrane, where they initiate changes in mitochondrial membrane potential (17, 18).

The biochemical pathways initiated by taxanes that lead to cell death are poorly understood and seem to vary between different types of cancer. Lymphoma cells treated with paclitaxel were reported to undergo death receptor–independent activation of caspase-8, which set up a mitochondrial amplification loop (8, 19). Studies on another lymphoblastic cell line implicated death receptor–independent activation of caspase-10 as the key event in paclitaxel-induced apoptosis (20).

In the present study, we examined the apoptosis-inducing potential of docetaxel in cultured melanoma cell lines and explored the biochemical pathways involved. The results indicate that apoptosis was caspase dependent and was mediated through the mitochondria. Activation of caspase-2 seemed to be the initiating event, whereas activation of caspase-8 was a delayed event resulting from activation of caspases.

Materials and Methods

Cell Lines

Human melanoma cell lines Me4405, Me1007, IgR3, Mel-FH, Mel-RM, Mel-CV, Mel-AT, SK-mel-28, SK-mel-110, and MM200 have been described previously (21). The cell lines were cultured in DMEM containing 5% FCS (Commonwealth Serum Laboratories, Melbourne, Australia).

Antibodies and Other Reagents

Docetaxel (Taxotere) was kindly provided by Aventis Pharma SA (Antony, France). Docetaxel was stored as a 100 mmol/L solution in absolute ethanol at −80°C and diluted with the DMEM before use. Recombinant human TRAIL was supplied by Immunex (Seattle, WA). The rabbit polyclonal antibodies against caspase-2, caspase-3, caspase-8, and caspase-9, and the mouse monoclonal antibodies against cytochrome *c* and poly(ADP)ribose polymerase (PARP) were purchased from PharMingen (Bioclone, Marrickville, Australia). The rabbit polyclonal anti-Bax against amino acids 1 to 20 was purchased from Upstate Biotechnology (Lake Placid, NY). Propidium iodide was purchased from Sigma-Aldrich (Castle Hill, NSW, Australia). The cell-permeable pan-caspase inhibitor Z-Val-Ala-Asp(OMe)-CH2F (z-VAD-fmk); the caspase-3–specific inhibitor Z-Asp(OMe)-Glu(OMe)-Val-Asp(OMe)-CH_2F (z-DEVD-fmk); the caspase-9–specific inhibitor Z-Leu-Glu(Ome)-His-Asp(Ome)-CH_2F (z-LEHD-fmk); the caspase-8–specific inhibitor Z-lle-Glu(Ome)-Thr-Asp(Ome)-CH_2F (z-IETD-fmk); the caspase-2–specific inhibitor Z-Val-Ala-Asp(OMe)-Val-Ala-Asp(OMe)-CH_2F (z-VDVAD-fmk); the mouse anti-Bak Ab-1 antibody; the caspase substrates z-VDVAD-AFC, z-DEVD-AFC, z-IETD-AFC, Ac-LEHD-AFC, to measure caspase-2, caspase-3, caspase-8, and caspase-9 activities, respectively; and the p53 inhibitor 2-(2-imino-4,5,6,7-tetrahydrobenzothiazol-3-yl)-1-(4-methylphenyl)ethanone (QB102) were purchased from Calbiochem (La Jolla, CA).

Apoptosis

Quantitation of apoptotic cells by measurement of sub-G_1 DNA content using the propidium iodide method was carried out as described elsewhere (22). Quantitation of apoptotic cells by Annexin V staining was carried out as described previously and according to the manufacturer's instructions (23).

In studies using QB102 (Calbiochem), a stock solution of 10 mmol/L was made by dissolving QB102 in DMSO, which was diluted with medium before use. Melanoma cells were pretreated with QB102 at 10 μmol/L for 3 h (24) before adding docetaxel for another 48 h. Cells were then collected and the percentage of apoptotic cells was determined using the propidium iodide method in flow cytometry.

Flow Cytometry

Immunostaining on intact and permeabilized cells was carried out as described previously (23). Analysis was carried out using a Becton Dickinson (Mountain View, CA) FACScan flow cytometer. The percentage of antigen-positive cells was calculated as the difference in positive area between the positive and negative control histograms. The positive area was that to the right of the intersection of the two curves (22).

Mitochondrial Membrane Potential ($\Delta\psi_m$)

Tumor cells were seeded at 1×10^5 per well in 24-well plates and allowed to reach exponential growth for 24 h before treatment. JC-1 staining was done according to the manufacturer's instructions (Molecular Probes, Eugene, OR). Briefly, adherent cells and nonadherent cells were collected and washed with PBS. Cells were then incubated with 10 μg/mL of JC-1 in warm PBS at 37°C for 15 min. After washing with PBS, the cells were analyzed using a FACScan flow cytometer (Becton Dickinson, Sunnyvale, CA). Cells with polarized mitochondria presented in the upper-right quadrant of the dot plot due to the formation of JC-1 aggregates, which emit orange fluorescence (590 nmol/L) when excited at 488 nmol/L. Cells with depolarized mitochondria emit green fluorescence (530 nmol/L) and are visualized in the lower-right quadrant in the dot plot (25).

Western Blot and Protein Expression Analysis

The protein content of cell extracts was determined by the Bradford assay (Bio-Rad, Regents Park, NSW, Australia). A total of 20 to 30 μg of protein were electrophoresed on 10% to 15% SDS-PAGE gels and transferred to nitrocellulose membranes. Membranes were blocked, incubated with primary antibodies at the appropriate concentration, and subsequently incubated with horseradish peroxidase–conjugated goat anti-rabbit IgG or goat anti-mouse IgG (1:3,000 dilutions; Bio-Rad). Labeled bands were detected by Immun-Star horseradish peroxidase chemiluminescent kit, and images were captured. The intensity of the bands was quantitated with the Bio-Rad VersaDoc image system (Bio-Rad). The relative expression of certain protein was determined by dividing the densitometric value of the test protein by that of the control [glyceraldehyde-3-phosphate dehydrogenase (GAPDH) or actin].

Caspase Activity Assay

The caspase substrates z-VDVAD-AFC, z-DEVD-AFC, z-IETD-AFC, and Ac-LEHD-AFC were used to measure caspase-2, caspase-3, caspase-8, and caspase-9 activities, respectively. Briefly, after incubation with docetaxel at 20 nmol/L for different time intervals, both the floating and adherent cells were collected, washed twice in ice-cold PBS, and lysed in 100 μL of caspase lysis buffer [25 mmol/L HEPES (pH 7.5), 5 mmol/L EDTA, 5 mmol/L $MgCl_2$, 10 mmol/L DTT, 10 μg/mL each of pepstatine and leupeptin, 0.5% Triton X-100, and 2 mmol/L phenylmethylsulfonyl fluoride]. Cells were kept on ice for 15 to 20 min with occasional mixing. The lysate was then centrifuged at 15,000 × *g* for 20 min at 4°C. Protein concentration of the supernatant was determined using the

Bradford method (bicinchoninic acid protein assay reagent). Subsequently, 40 μg of sample were diluted into a final volume of 200 μL with the assay buffer (50 mmol/L HEPES, 10% sucrose, 0.1% CHAPS, and 10 mmol/L DTT) containing the fluorogenic caspase substrate at a final concentration of 100 μmol/L and incubated for 1 to 2 h in a 96-well plate at 30°C. The generation of free AFC was determined by fluorescence measurement using Fluostar OPTIMA (LABTECH, Offenburg, Germany) set at an excitation wavelength of 400 nm and an emission wavelength of 505 nm.

Plasmid Vector and Transfection

Stable Mel-RM transfectants of Bcl-2 were established by electroporation of the PEF-puro vector carrying human Bcl-2 provided by Dr. David Vaux (Walter and Eliza Hall Institute, Melbourne, Victoria, Australia) and described elsewhere (26).

Preparation of Mitochondrial and Cytosolic Fractions

Methods used for subcellular fraction were similar to the methods described previously (22).

SiRNA-Mediated Silencing of Caspase-2, Noxa, and PUMA

Cells were transfected in six-well plates with caspase-2–, Noxa-, or PUMA-specific or nontarget control small interfering RNA (siRNA) constructs (Dharmacon, Lafayette, CO) for 24 h according to the manufacturer's protocol. The construct used was the siRNA SMARTpool caspase-2, Noxa, or PUMA. Cells were transfected with 100 nmol/L of the above siRNA using LipofectAMINE (Invitrogen, Carlsbad, CA) according to the manufacturer's protocol. Following silencing, cells were treated for another 24 or 48 h with or without docetaxel at 20 nmol/L, and apoptotic cells were quantified by the propidium iodide method in flow cytometry. Efficiency of RNA interference was assessed by immunoblotting.

Statistical Analysis

Data are expressed as mean ± ISE. The statistical significance of intergroup differences in normally distributed continuous variables was determined using Student's *t* test. *P* values >0.05 were considered statistically significant.

Results

Docetaxel-Induced Apoptosis of Melanoma Cells

We examined the apoptosis-inducing potential of docetaxel in melanoma cells by treating two melanoma cell lines, IgR3 and MM200, with a range of docetaxel concentrations as follows: 0, 1, 2.5, 5, 10, 20, 40, and 80 nmol/L for 24 h. As shown in Fig. 1A, docetaxel induced apoptosis of the melanoma cells in a dose-dependent manner, with the highest percentage of apoptotic cells seen

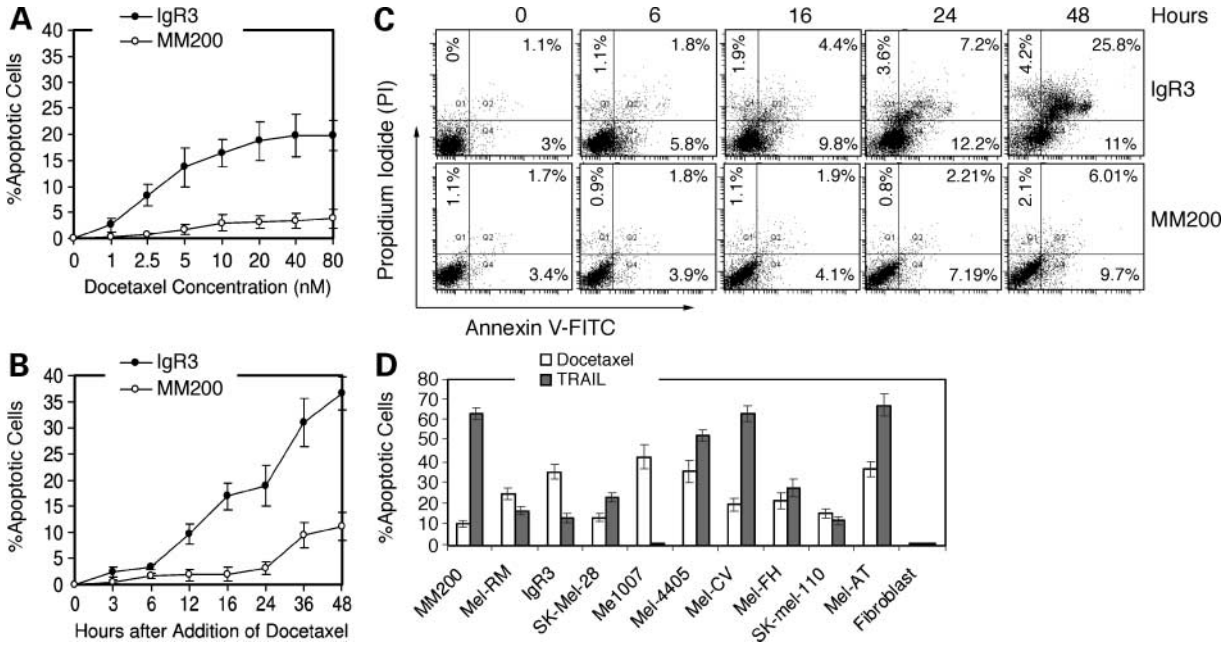

Figure 1. Docetaxel-induced apoptosis of melanoma cells. **A,** titration of docetaxel on induction of apoptosis. IgR3 and MM200 cells were treated with docetaxel at indicated doses for 24 h before measurement of apoptosis by the propidium iodide method using flow cytometry. *Points,* mean of three individual experiments; *bars,* ISE. **B,** kinetics of induction of apoptosis by docetaxel. IgR3 and MM200 cells were treated with docetaxel at 20 nmol/L for the indicated time periods before measurement of apoptosis by the propidium iodide method using flow cytometry. *Points,* mean of three individual experiments; *bars,* ISE. **C,** representative dot plots showing fluorescence channel analyses of melanoma cells after dual staining with Annexin V and propidium iodide. IgR3 and MM200 cells were treated with docetaxel at 20 nmol/L for the indicated time periods and then stained with FITC-conjugated Annexin V (*green fluorescence, horizontal axis*) and propidium iodide (*red fluorescence, vertical axis*) and analyzed using flow cytometry. Annexin V binding to phosphatidylserine in the absence of propidium iodide staining is indicative of early apoptosis. Representative of three individual experiments. **D,** docetaxel-induced apoptosis in a panel of melanoma cell lines but not in normal fibroblasts. Cells were treated with either TRAIL at 200 ng/mL or docetaxel at 20 nmol/L for 24 and 48 h, respectively, and apoptosis was measured by the propidium iodide method using flow cytometry. *Columns,* mean of three individual experiments; *bars,* ISE.

at 20 to 40 nmol/L. Figure 1B indicates that apoptosis of IgR3 cells was detected after 3 h of treatment and peaked at 36 to 48 h. This concentration seems clinically relevant based on the reported plasma concentration of docetaxel in patients treated with docetaxel (27).

Dual staining with Annexin V and propidium iodide shown in Fig. 1C indicated that reactivity with Annexin V preceded the staining with propidium iodide, consistent with induction of apoptosis rather than necrosis. For example, only 4.2% of the sensitive IgR3 cells stained with propidium iodide alone at 48 h. A summary of studies of docetaxel on a panel of melanoma cell lines is illustrated in Fig. 1D. TRAIL, known to induce apoptosis in two thirds of melanoma cells (23), was used as a positive control (200 ng/mL for 16 h). Results showed that there was very little concordance between the degree of apoptosis induced by TRAIL and docetaxel in the melanoma cell lines.

Docetaxel Induces Caspase-Dependent Apoptosis in Melanoma Cells

To assess the role of caspases in docetaxel-induced apoptosis, IgR3 and MM200 cells were pretreated with the pan-caspase inhibitor z-VAD-fmk (20 μmol/L), or specific inhibitors of caspase-2, z-VDVAD-fmk (50 μmol/L), caspase-3, z-DEVD-fmk (30 μmol/L), caspase-8, z-IETD-fmk (30 μmol/L), or caspase-9, z-LEHD-fmk (30 μmol/L). The inhibitors were added 1 h before adding TRAIL (200 ng/mL) or docetaxel (20 nmol/L) for another 24 and 48 h, respectively. As shown in Table 1, the pan-caspase inhibitor z-VAD-fmk significantly reduced docetaxel-induced apoptosis. Inhibition of docetaxel-induced apoptosis by the specific inhibitors was most marked with that against caspase-2 and caspase-9 in studies on the sensitive IgR3 melanoma cell line. Inhibitor of caspase-8 had very little effect. All the inhibitors had a low level of activity against the low killing of the MM200 cell line.

Table 1. Effect of caspase inhibitors on docetaxel-induced apoptosis of melanoma cells

Cell line†	Percentage inhibition*			
	IgR3		MM200	
Caspase inhibitor	Docetaxel	TRAIL	Docetaxel	TRAIL
No inhibitor‡	35.5 ± 3.2	11.3 ± 1.9	10.3 ± 1.8	67.8 ± 4.61
z-VAD-fmk	67 ± 3.1	97 ± 1.2	27 ± 2.1	98.2 ± 0.98
z-VDVAD-fmk	56 ± 2.4	68 ± 4.21	23 ± 1.7	43.1 ± 3.1
z-DEVD-fmk	37 ± 2.89	98 ± 1.1	25 ± 2	72.1 ± 3.98
z-IETD-fmk	12.6 ± 2.9	98 ± 0.78	19 ± 1.9	82 ± 4.1
z-LEHD-fmk	45 ± 3.16	98 ± 1	19.3 ± 1.2	87 ± 3.67

*Data are the mean ± SE of three individual experiments.

†IgR3 and MM200 cells were pretreated with the pan-caspase inhibitor z-VAD-fmk (20 μmol/L), the caspase-2 inhibitor z-VDVAD-fmk (50 μmol/L), the caspase-3 inhibitor z-DEVD-fmk (30 μmol/L), the caspase-8 inhibitor z-IETD-fmk (30 μmol/L), or the caspase-9 inhibitor z-LEHD-fmk (30 μmol/L), 1 h before adding TRAIL (200 ng/mL) or docetaxel (20 nmol/L) for another 24 and 48 h, respectively. Apoptosis was measured by the propidium iodide method using flow cytometry.

‡Apoptosis level induced by docetaxel and TRAIL.

The involvement of caspases in docetaxel-induced apoptosis was further examined by Western blot analysis before and after exposure to docetaxel. The kinetics of caspase activation in the two cell lines is shown in Fig. 2A. In IgR3 cells, cleavage of caspase-2 was evident by 12 h, whereas cleavage of caspase-9 and caspase-3 was evident by 16 h. Cleavage of PARP was evident by 16 h. Activation of caspase-8 was only evident at 24 to 36 h. In MM200 cells, cleavage of caspase-3, caspase-9, and PARP was detectable only at 24 to 36 h. Figure 2A also shows the effect of treatment with docetaxel on X-linked inhibitor of apoptosis expression, which was reported to be cleaved by activated caspase-3 (28). Reduction in density of the X-linked inhibitor of apoptosis protein bands was evident in the sensitive cell line IgR3 by 16 to 36 h but not in the resistant MM200 cells.

Previous studies suggested that caspase-2 can act upstream of mitochondria and induce cytochrome *c* and AIF release (29–31). To examine whether caspase-2 is required for docetaxel-induced apoptosis, we assessed the kinetics of activation of caspase-2, caspase-8, and caspase-9 and the effector caspase-3 using the caspase fluorogenic substrates z-VDVAD-AFC, z-DEVD-AFC, z-IETD-AFC, and z-LEHD-AFC to measure caspase-2, caspase-3, caspase-8, and caspase-9 activities, respectively (Fig. 2B). Caspase-2 appeared to be activated first and to a higher degree compared with other caspases at 3 h after treatment of IgR3 cells with docetaxel. Activated caspase-3 correlated well with activated caspase-9. Activation of caspase-8 was delayed and became active after caspase-3 activation, indicating that caspase-8 was unlikely to be an initiator of docetaxel-induced apoptosis.

Docetaxel Activates the Mitochondrial Apoptotic Pathway

To identify the apoptotic pathway being activated in response to docetaxel, we measured the mitochondrial membrane potential in melanoma cells treated with docetaxel for different time periods. Changes in mitochondrial membrane potential were studied using a fluorescent cationic dye 5,5′,6,6′-tetrachloro-1,1′,3,3′-tetraethyl-benzamidazolocarbocyanin iodide, known as JC-1. In healthy cells, JC-1 exists as a monomer in the cytosol (FL1-positive; green) and also accumulates as aggregates in the mitochondria (FL2-positive; red). In apoptotic cells, JC-1 exists exclusively in monomer form and produces a green cytosolic signal (32). As shown in Fig. 2C, docetaxel induced mitochondrial depolarization detected at 12 h in both IgR3 and MM200 cells and peaked at 48 h. Reduction in mitochondrial membrane potential was at low levels in MM200 cells compared with that in IgR3 cells.

Docetaxel-induced mitochondrial membrane potential changes were further examined by studying the release of cytochrome *c* and apoptosis-inducing factor (AIF) from the mitochondria to the cytosol in both sensitive and

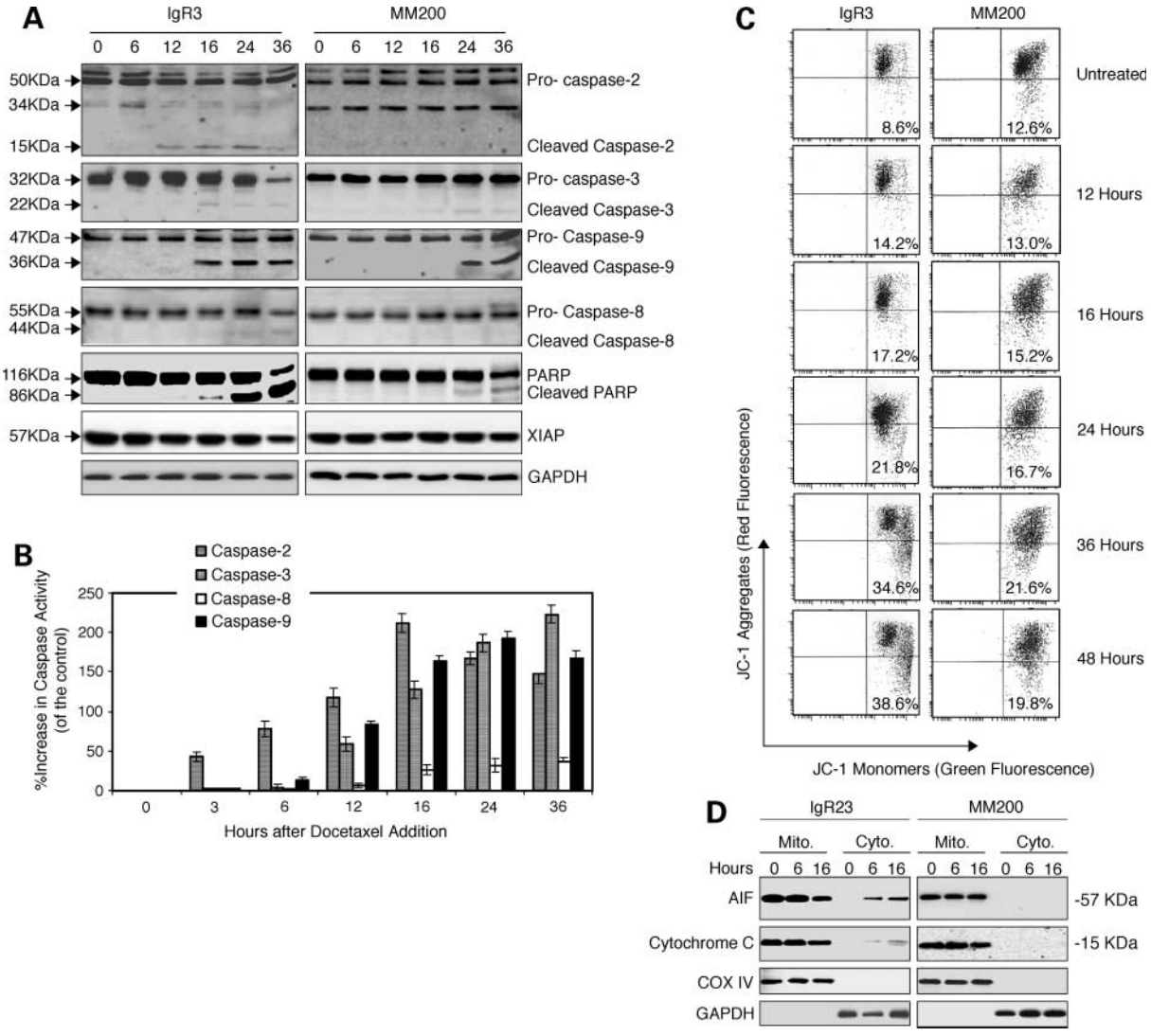

Figure 2. Activation of caspases by docetaxel and cleavage of the caspase-3 substrates, PARP, and X-linked inhibitor of apoptosis. **A,** IgR3 and MM200 cells were treated with docetaxel at 20 nmol/L for the indicated time periods. Whole-cell lysates were subjected to Western blot analysis. Western blot analysis of GAPDH levels was included to show that equivalent amounts of protein were loaded in each lane. Representative of two individual experiments. **B,** caspase-2 is activated before other initiating caspase-8 and caspase-9. IgR3 cells were treated with docetaxel at 20 nmol/L for the indicated time points before cell lysate was analyzed for caspase activation using caspase-specific fluorescent AFC substrates. The percentage of increase of caspase activity was calculated as the increase in AFC fluorescence with docetaxel treatment minus background fluorescence divided by AFC fluorescence without docetaxel treatment minus the background. *Columns,* mean of three individual experiments; *bars,* ISE. **C,** docetaxel induces changes in mitochondrial membrane potential. IgR3 and MM200 cells were treated with docetaxel at 20 nmol/L for the indicated time periods followed by measurement of $\Delta\psi_m$ using JC-1 in flow cytometry. *Numbers in bottom, right,* percentage of cells with reduced mitochondrial potential as indicated by disappearance of JC-1 aggregates (*red fluorescence, top, right*) and appearance of JC-1 monomers. Representative of three individual experiments. **D,** docetaxel induces the release of AIF and cytochrome *c* from mitochondria to the cytosol. IgR3 and MM200 cells were treated with docetaxel at 20 nmol/L for 6 and 16 h before harvest. Mitochondrial and cytosolic fractions were subjected to Western blot analysis. Western blot analysis of cyclooxygenase IV (*COX IV*) levels was included to show relative purity of mitochondrial fractions. Western blot analysis of GAPDH levels was included as a cytosolic marker. Representative of two individual experiments.

resistant melanoma cells. As shown in Fig. 2D, cytochrome *c* and AIF were located exclusively in the mitochondrial fractions before treatment with docetaxel and were released to cytosol after exposure to docetaxel in IgR3 but not MM200 cells. The release of AIF preceded the release of cytochrome *c* that was delayed up to 16 h after treatment with docetaxel.

Docetaxel Promotes Activation of Bax and Bak

The proapoptotic Bcl-2 family proteins, Bax and Bak, are activated by conformational changes induced by a variety of stimuli (33, 34) and can be detected in permeabilized cells using antibodies that recognize only the activated forms of Bax (35) or Bak (clone Ab-1; ref. 34). Figure 3A shows a marked increase in the levels of conformationally

changed Bax and Bak in IgR3, which started at 6 h for Bax and 12 h for Bak and peaked at 36 h of treatment with docetaxel. In contrast, activated Bax and Bak appeared later in MM200 cells at 24 h, and changes were maximal at 36 to 48 h.

We examined the expression of Bax in different subcellular fractions of IgR3 and MM200 cells with or without exposure to docetaxel. As shown in Fig. 3B, the Bax protein was predominantly located in the cytosol before treatment with docetaxel. In contrast, after treatment with docetaxel for 16 h, Bax was observed in the mitochondrial fractions with corresponding decrease in the levels of expression in the cytosol. This was most evident in the docetaxel-sensitive IgR3 cells.

Overexpression of Bcl-2 Inhibits Docetaxel-Induced Apoptosis in Melanoma Cells

To investigate whether the observed mitochondrial dysfunction is required for docetaxel-induced apoptosis, we transfected cDNA encoding Bcl-2 into Mel-RM cells as shown in Fig. 3C. There was a marked increase in the levels of Bcl-2 in the Bcl-2–transfected cells, but the levels in the cells transfected with the vector alone were similar to those in the parental cells. Apoptosis of melanoma induced by TRAIL, which is known to induce apoptosis of melanoma predominantly through the mitochondrial apoptotic pathway, was almost completely inhibited in the Bcl-2 transfectants. Similarly, the levels of docetaxel-induced apoptosis in Bcl-2–transfected cells were markedly decreased compared with those in vector alone–transfected cells. As shown in Fig. 3D, docetaxel-induced changes in the mitochondrial membrane potential were reversed in Bcl-2–transfected cells but not in cells transfected with the vector alone. Similarly, docetaxel-induced caspase-3 activation and Bak conformational changes were inhibited by Bcl-2 overexpression. Docetaxel-induced Bax conformational changes were not affected in Bcl-2–overexpressing cells.

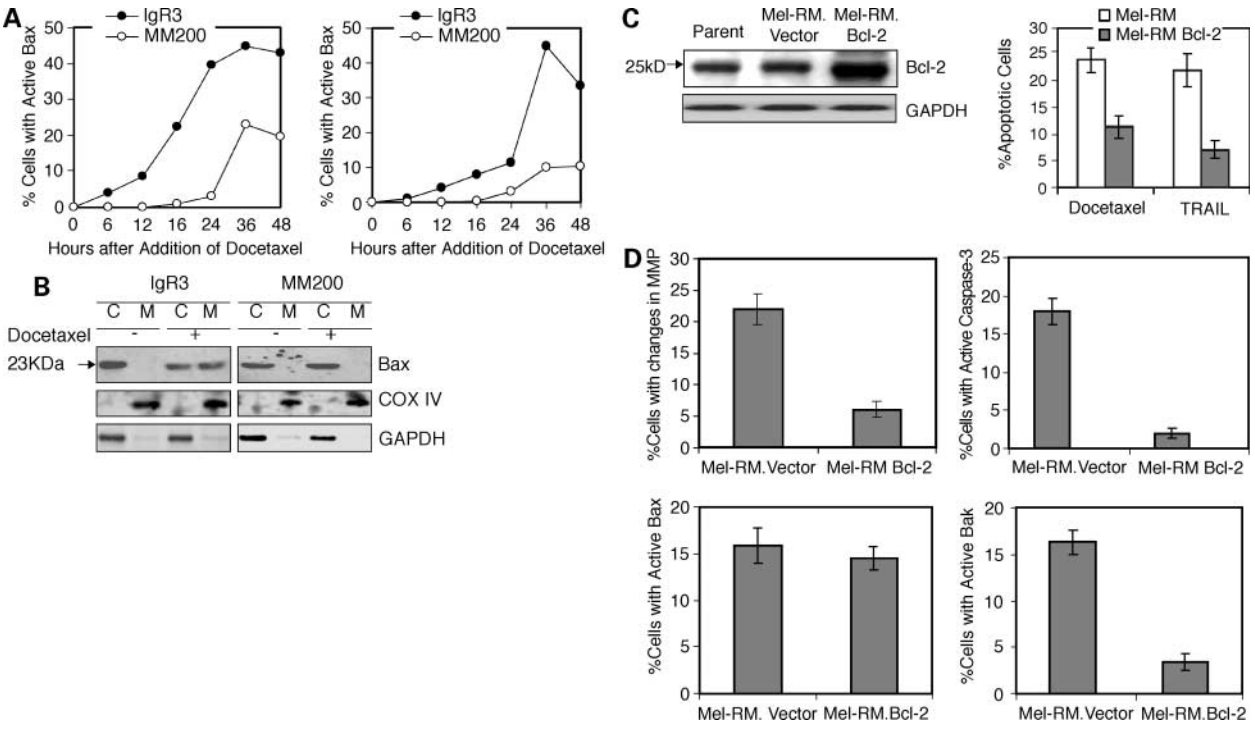

Figure 3. Docetaxel activates the mitochondrial apoptosis pathway. **A,** docetaxel induces conformational changes of Bax and Bak. IgR3 and MM200 cells were treated with or without docetaxel at 20 nmol/L for the indicated time periods before being subjected to flow cytometry analysis using either a Bax NH_2-terminal epitope-specific antibody or anti-Bak Ab-1 that specifically recognize activated forms of Bax or Bak, respectively. Representative of three individual experiments. **B,** docetaxel induces Bax relocation from the cytosol to mitochondria. IgR3 and MM200 cells were treated with docetaxel for 16 h before harvest. The mitochondrial and cytosolic fractions were subjected to Western blot analysis. Western blot analysis of cyclooxygenase IV and GAPDH levels was included as controls. Representative of two individual experiments. **C,** overexpression of Bcl-2 inhibits docetaxel-induced apoptosis. *Left,* Bcl-2 was overexpressed in Mel-RM cells transfected with the cDNA encoding Bcl-2, but not in the cells transfected with the vector alone. Whole-cell lysates were subjected to Western blot analysis. Western blot analysis of GAPDH levels was included to show that equivalent amounts of protein were loaded in each lane. Representative of two individual experiments. *Right,* Mel-RM cells transfected with c-DNA for Bcl-2 or vector alone were treated with either TRAIL at 200 ng/mL or docetaxel at 20 nmol/L for 24 and 48 h, respectively, before measurement of apoptosis by the propidium iodide method using flow cytometry. *Columns,* mean of three individual experiments; *bars,* ISE. **D,** overexpression of Bcl-2 inhibited docetaxel-induced $\Delta\psi_m$ changes, caspase-3 activation, and conformational changes of Bak but not Bax. Mel-RM cells transfected with cDNA for Bcl-2 or vector alone were treated with docetaxel at 20 nmol/L for 24 h. The changes in $\Delta\psi_m$ were measured by JC-1 using flow cytometry. Activated forms of caspase-3, Bax, and Bak were measured in flow cytometry using a monoclonal antibody that recognizes the processed caspase-3, a Bax NH_2-terminal epitope-specific antibody, or anti-Bak Ab-1, respectively. *Columns,* mean of three individual experiments; *bars,* ISE.

Premitochondrial Caspase-2 Activation Is Required for Docetaxel-Induced Apoptosis

To explore the role of caspase-2 in docetaxel-induced apoptosis, z-VDVAD-fmk, a specific inhibitor of caspase-2, was used. As shown in Fig. 4A, inhibition of caspase-2 significantly impaired mitochondrial membrane potential changes induced by docetaxel and decreased release of AIF (by 49% of that induced by docetaxel alone) and cytochrome *c* (by 52%) from the mitochondria. Consistent with these results, cleavage of pro-caspase-9, pro-caspase-3, and PARP was markedly reduced after pretreatment with the caspase-2 inhibitor (Fig. 4B). Caspase-2 seemed to act upstream of activation of the multidomain proteins Bax and Bak. Caspase-2 inhibitor reduced activation of both Bax and Bak and inhibits Bax translocation to mitochondria (Fig. 4C). Furthermore, inhibition of caspase-2 using a siRNA specific for caspase-2 resulted in a marked inhibition of docetaxel-induced apoptosis (Fig. 4D).

Docetaxel-Induced Apoptosis Is Independent of p53

Previous studies have shown that caspase-2 may be activated by a complex of a p53-induced death domain containing protein and an adaptor protein RAIDD (36). In view of this, we examined activation of p53 in IgR3 and MM200 cell lines by Western blots and used an inhibitor of p53 to determine its possible role in docetaxel-induced activation. Our results showed that p53 levels were increased by 16 h in the resistant MM200 cells, but p53 did not undergo significant change in the sensitive IgR3 cells (Fig. 5A). ME4405 cells do not express p53 but were sensitive to docetaxel (data are not shown). Noxa and PUMA are known targets of p53. Noxa was up-regulated in both cell lines from 6 to 24 h, and PUMA was up-regulated in both cells by 16 h. Knockdown of these proteins individually by siRNA, however, did not decrease docetaxel-induced apoptosis of the sensitive IgR3 line (Fig. 5B). Combining siRNA for both Noxa and PUMA also did not decrease docetaxel-induced apoptosis (data not shown).

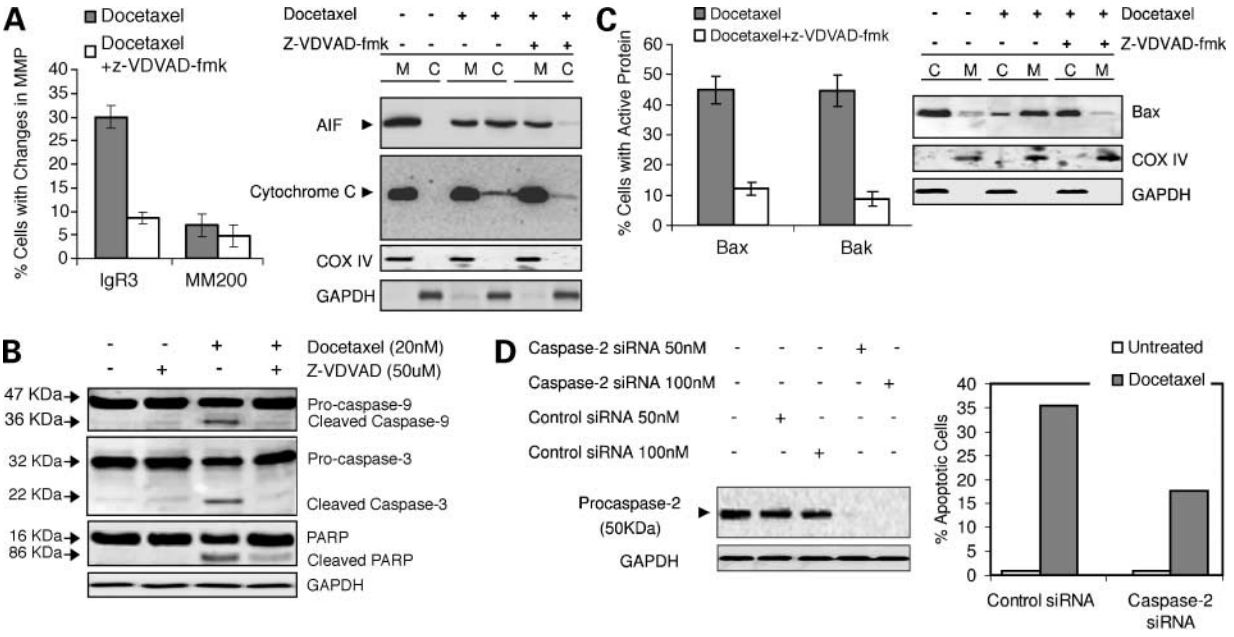

Figure 4. Caspase-2 is activated upstream of mitochondria, caspase-9, and caspase-3. **A,** caspase-2 is upstream of the mitochondrial membrane changes (*left*). IgR3 and MM200 cells were treated with or without the caspase-2 inhibitor z-VDVAD-fmk for 1 h before the addition of docetaxel at 20 nmol/L for another 48 h, followed by measurement of $\Delta\psi_m$ by JC-1 using flow cytometry. *Columns,* mean of three individual experiments; *bars,* ISE. Docetaxel-induced release of AIF and cytochrome *c* is suppressed by caspase-2 inhibition (*right*). IgR3 cells with or without pretreatment with caspase-2 inhibitor for 1 h were treated with docetaxel at 20 nmol/L for 16 h. Mitochondrial (*M*) and cytosolic (*C*) fractions were subjected to Western blot analysis. Western blot of cyclooxygenase IV levels was included to show relative purity of the mitochondrial fractions. Western blot analysis of GAPDH levels was included as a cytosolic marker. Representative of two individual experiments. **B,** caspase-2 is upstream of caspase-9, caspase-3 activation, and PARP cleavage. IgR3 cells with or without pretreatment with the caspase-2 inhibitor z-VDVAD-fmk for 1 h were treated with docetaxel at 20 nmol/L for 16 h. Whole-cell lysates were subjected to Western blot analysis. Western blot analysis of GAPDH levels was included to show that equivalent amounts of protein were loaded in each lane. Representative of two individual experiments. **C,** caspase-2 is upstream of Bax and Bak activation. Inhibition of caspase-2 suppresses conformational changes of Bax and Bak (*left*). IgR3 cells with or without pretreatment with the caspase-2 inhibitor z-VDVAD-fmk at 50 μmol/L for 1 h were treated with docetaxel at 20 nmol/L for 36 h before flow cytometry analysis using a Bax NH_2-terminal epitope-specific antibody or anti-Bak Ab-1. Representative of three individual experiments. *Right,* inhibition of caspase-2 suppresses Bax relocation from the cytosol to mitochondria. IgR3 cells with or without pretreatment with the caspase-2 inhibitor z-VDVD-fmk for 1 h were treated with docetaxel at 20 nmol/L for 16 h before harvest. The mitochondrial and cytosolic fractions were subjected to Western blot analysis. Cyclooxygenase IV and GAPDH levels were included as controls as described above. Representative of two individual experiments. **D,** down-regulation of caspase-2 expression in IgR3 cells inhibits docetaxel-induced apoptosis. IgR3 cells were transfected with caspase-2 – specific siRNA sequence (Dharmacon) for 24 h. The whole-cell lysates were subjected to Western blot analyses (*left*). Transfected cells were exposed to docetaxel for 48 h and assessed for apoptosis using the propidium iodide method (*right*). Representative of two individual experiments.

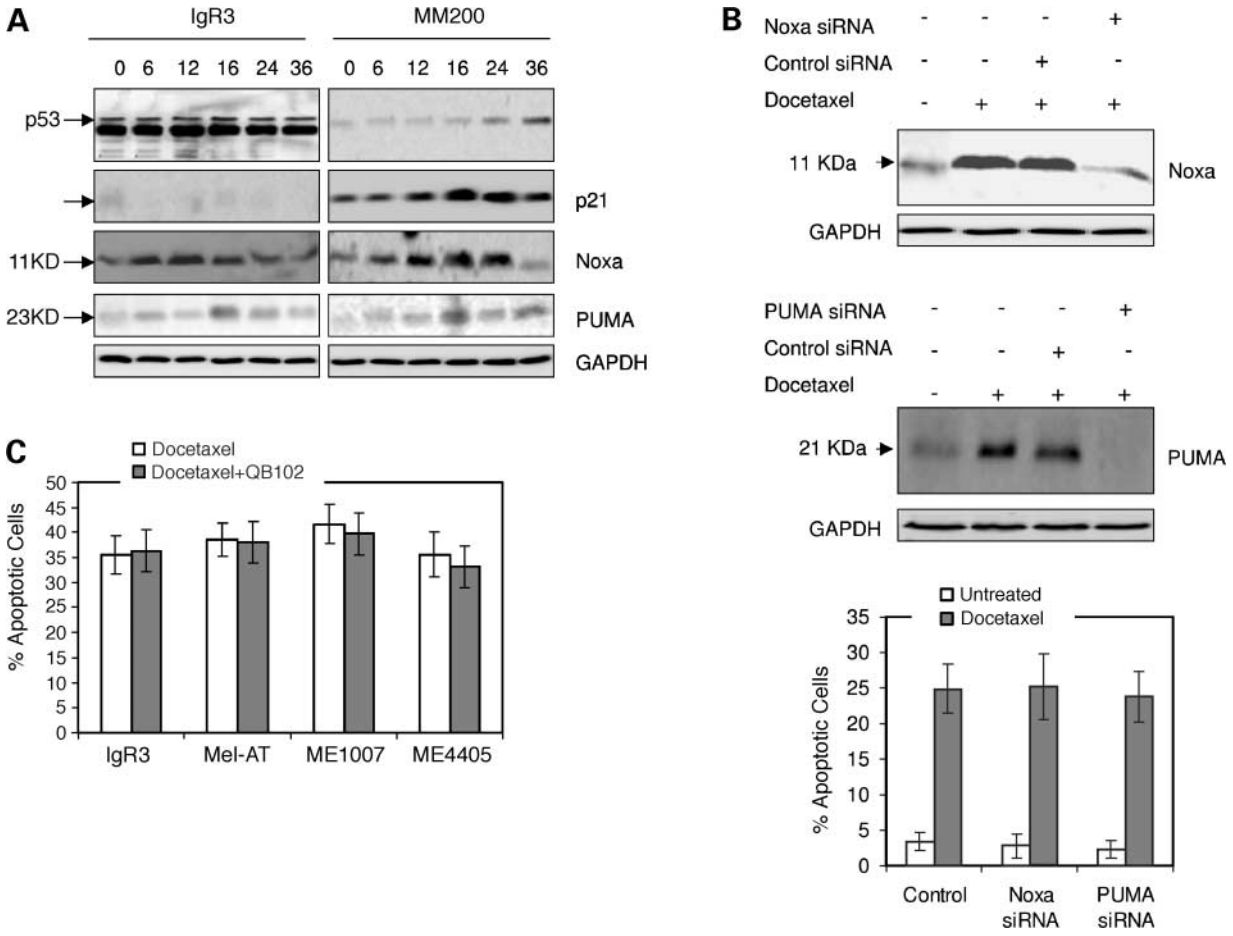

Figure 5. Docetaxel-induced apoptosis does not involve p53 activation. **A,** IgR3 and MM200 cells were treated with docetaxel at 20 nmol/L for the indicated time periods and whole-cell lysates were subjected to Western blot analysis. Docetaxel did not induce changes in p53 protein levels in the sensitive IgR3 cells, whereas p53 and p21 was up-regulated in the resistant MM200 cells. GAPDH blot was included to show that equivalent amounts of protein were loaded in each lane. Representative of two individual experiments. **B,** down-regulation of Noxa or PUMA expression in IgR3 cells does not affect docetaxel-induced apoptosis. IgR3 cells were transfected with either Noxa- or PUMA-specific siRNA sequence (Dharmacon) for 24 h. Cells were then treated with or without docetaxel for another 16 h and whole-cell lysates were subjected to Western blot analyses (*left*), or were exposed to docetaxel for 24 h and assessed for apoptosis using the propidium iodide method (*right*). Representative of three individual experiments. *Columns,* mean of three individual experiments; *bars,* ISE. **C,** inhibition of p53 does not protect melanoma cells against docetaxel-induced apoptosis. IgR3, Me1007, and Mel-AT cells were treated with the p53 inhibitor QB102 at 10 μmol/L 3 h before adding docetaxel at 20 nmol/L for another 48 h. Apoptosis was measured by the propidium iodide method using flow cytometry. *Columns,* means of three individual experiments; *bars,* ISE.

To further examine the role of p53, we used QB102, a chemical inhibitor of p53, which is able to inhibit p53-dependent apoptosis by reversible inhibition of both p53 transactivation activity and p53 downstream events (24). In our studies, QB102 at 10 μmol/L was able to inhibit cisplatin-induced p53 up-regulation and its downstream gene *p21* in melanoma cells (data not shown). IgR3, Mel-AT, ME4405, and ME1007 were pretreated with QB102 at 10 μmol/L for 3 h before adding docetaxel for another 48 h. As shown in Fig. 5C, p53 inhibition did not protect melanoma cells against docetaxel-induced apoptosis.

Discussion

In the present study, we show that docetaxel induced varying degrees of apoptotic cell death in a panel of melanoma cell lines but did not induce apoptosis in normal fibroblasts. Apoptosis induced in melanoma cells included those that were resistant to TRAIL, a member of the tumor necrosis factor family that induces apoptosis in about two thirds of melanoma cell lines (23). In contrast to TRAIL-induced apoptosis (22), docetaxel-induced apoptosis of melanoma proceeded much more slowly (3–48 h) and seemed to involve activation of caspase-2 as the initiating caspase. This was shown by early activation of caspase-2 compared with other caspases using Western blot and fluorogenic substrate assays for caspase-2, caspase-3, caspase-8, and caspase-9. Moreover, inhibition of caspase-2 by z-VDVAD-fmk or by siRNA knockdown significantly protected melanoma cells from docetaxel-induced apoptosis. Apoptosis seemed to proceed via the mitochondrial pathway, as shown by changes in mitochondrial membrane

potential associated with release of AIF and cytochrome *c*, activation of caspase-9 and caspase-3, and cleavage of PARP. Moreover, docetaxel-induced apoptosis was inhibited by overexpression of Bcl-2 in melanoma cells.

Analysis of changes in the multidomain proapoptotic proteins Bax and Bak by flow cytometry revealed that treatment with docetaxel resulted in conformational changes in both proteins that correlated with the onset of docetaxel-induced apoptosis. These changes were not inhibited by overexpression of Bcl-2, suggesting that they were upstream of the mitochondria. Importantly, inhibition of caspase-2 with z-VDVAD-fmk prevented docetaxel-induced changes in Bax, indicating that changes in caspase-2 were responsible for conformational changes in Bax.

Several previous studies have also suggested that caspase-2 is an apical caspase for stress-induced apoptosis via activation of Bax (29, 37). The mechanisms involved, however, were not clear. Caspase-2 has a caspase recruitment domain prodomain, which can associate with RAIDD, an adaptor protein containing a caspase recruitment domain and death domain (38). RAIDD was proposed to interact with PIP1 and thereby to link tumor necrosis factor receptor 1 activation with caspase-2–mediated apoptosis (38, 39). More recently, caspase-2 was shown to be recruited to the DISC complex in T and B cells but did not initiate apoptosis mediated through Fas (40). Paroni et al. (41) suggested that caspase-2 was able to trigger mitochondrial dysfunction in response to genotoxic agents, in complex with the p53-induced death domain–containing protein and the adaptor protein RAIDD (36).

Several of these proposed mechanisms, such as involvement of death receptors, seem unlikely to explain its role in docetaxel-induced killing in that melanoma cells deficient in caspase-8 (Me-1007) or Bid (IgR3) were sensitive to the agent. Mechanisms dependent on activation of p53 also did not seem to be involved as p53 did not undergo significant increases in response to docetaxel in the sensitive IgR3 cells. ME4405 cells, which do not contain p53, were sensitive to docetaxel. Inhibition of p53 activation with QB102, a chemical that reversibly blocks p53-dependent transactivation of p53-responsive genes and inhibits p53-mediated apoptosis (24), was unable to protect melanoma cells against docetaxel-induced apoptosis. We detected up-regulation of the p53-dependent protein Noxa and PUMA, but siRNA knockdown studies of these proteins had no effect on docetaxel-induced apoptosis. Studies on cortical neurons reported cytoprotective mechanisms in which Bax specifically interacted with certain proteins that suppressed Bax translocation. It was proposed that caspase-2 could inhibit this interaction and allow Bax to be relocated to mitochondria (42, 43).

In summary, docetaxel-induced apoptosis of melanoma cells seems to depend largely on activation of caspase-2, which induces conformational changes in Bax and subsequent events leading to apoptosis. To our knowledge, this is the first study to identify caspase-2 as an important mediator of apoptosis induced by taxanes in melanoma. Whether the same mechanism applies against fresh isolates of melanoma is yet to be determined but if substantiated in such isolates, the present studies may provide valuable insights into the basis for sensitivity or resistance of melanoma to docetaxel. As reported elsewhere, cisplatin induces more rapid apoptosis of melanoma through the mitochondrial pathway (44). However, apoptosis induced by cisplatin or by vincristine does not involve caspase-2,[1] suggesting that the taxanes induce apoptosis by different mechanism to these drugs. These and ongoing studies promise to provide valuable insights that may assist in more effective use of the taxanes in treatment of melanoma.

[1] In preparation.

References

1. Soengas MS, Lowe SW. Apoptosis and melanoma chemoresistance. Oncogene 2003;22:3138 – 51.
2. Hersey P, Zhang X. How melanoma cells evade TRAIL-induced apoptosis. Nat Rev Cancer 2001;1:142 – 50.
3. Hersey P, Zhang XD. Overcoming resistance of cancer cells to apoptosis. J Cell Physiol 2003;196:9 – 18.
4. Debatin KM, Poncet D, Kroemer G. Chemotherapy: targeting the mitochondrial cell death pathway. Oncogene 2002;21:8786 – 803.
5. Lewanski CR, Gullick WJ. Radiotherapy and cellular signalling. Lancet Oncol 2001;2:366 – 70.
6. Wesselborg S, Engels IH, Rossmann E, Los M, Schulze-Osthoff K. Anticancer drugs induce caspase-8/FLICE activation and apoptosis in the absence of CD965 receptor/ligand interaction. Blood 1999;93: 3053 – 63.
7. Rowinsky EK, Donehower RC. The clinical pharmacology and use of antimicrotubule agents in cancer chemotherapeutics. Pharmacol Ther 1991;52:35 – 84.
8. Goncalves A, Braguer D, Carles G, Andre N, Prevot C, Briand C. Caspase-8 activation independent of CD95/CD95-L interaction during paclitaxel-induced apoptosis in human colon cancer cells (HT29-D4). Biochem Pharmacol 2000;60:1579 – 84.
9. Bhalla KN. Microtubule-targeted anticancer agents and apoptosis. Oncogene 2003;22:9075 – 85.
10. Gogas H, Bafaloukos D, Bedikian AY. The role of taxanes in the treatment of metastatic melanoma. Melanoma Res 2004;14:415 – 20.
11. Rao RD, Holtan SG, Ingle JN, et al. Combination of paclitaxel and carboplatin as second-line therapy for patients with metastatic melanoma. Cancer 2006;106:375 – 82.
12. Liu X, Kim CN, Yang J, Jemmerson R, Wang X. Induction of apoptotic program in cell-free extracts: requirement for dATP and cytochrome *c*. Cell 1996;86:145 – 57.
13. Susin SA, Lorenzo HK, Zamzami N, et al. Mitochondrial release of caspase-2 and -9 during the apoptotic process. J Exp Med 1999;189: 381 – 93.
14. Du C, Fang M, Li Y, Li L, Wang X. Smac, a mitochondrial protein that promotes cytochrome *c*-dependent caspase activation by eliminating IAP inhibition. Cell 2000;102:33 – 42.
15. Verhagen AM, Ekert PG, Pakusch M, et al. Identification of DIABLO, a mammalian protein that promotes apoptosis by binding to and antagonizing IAP proteins. Cell 2000;102:43 – 53.
16. Hegde R, Srinivasula SM, Zhang Z, et al. Identification of Omi/HtrA2 as a mitochondrial apoptotic serine protease that disrupts inhibitor of apoptosis protein-caspase interaction. J Biol Chem 2002;277: 432 – 8.
17. Cheng EH, Wei MC, Weiler S. BCL-2, BCL-X(L) sequester BH3 domain-only molecules preventing BAX- and BAK-mediated mitochondrial apoptosis. Mol Cell 2001;8:705 – 11.
18. Bouillet P, Strasser A. BH3-only proteins—evolutionarily conserved

proapoptotic Bcl-2 family members essential for initiating programmed cell death. J Cell Sci 2002;115:1567 – 74.

19. von Haefen C, Wieder T, Essmann F, Schulze-Osthoff K, Dorken B, Daniel PT. Paclitaxel-induced apoptosis in BJAB cells proceeds via death receptor-independent, caspase-3/8-driven mitochondrial amplification loop. Oncogene 2003;22:2236 – 47.

20. Park SJ, Wu CH, Gordon JD, Zhong X, Emami A, Safa AR. Taxol induces caspase-10-dependent apoptosis. J Biol Chem 2004;279:51057 – 67.

21. Zhang XD, Borrow JM, Zhang XY, Nguyen T, Hersey P. Activation of ERK1/2 protects melanoma cells from TRAIL-induced apoptosis by inhibiting Smac/DIABLO release from mitochondria. Oncogene 2003;22: 2869 – 81.

22. Zhang XD, Zhang XY, Gray CP, Nguyen T, Hersey P. Tumor necrosis factor-related apoptosis-inducing ligand-induced apoptosis of human melanoma is regulated by Smac/DIABLO release from mitochondria. Cancer Res 2001;61:7339 – 48.

23. Zhang XD, Franco A, Myers K, et al. Relation of TNF-related apoptosis-inducing ligand (TRAIL) receptor and FLICE-inhibitory protein expression to TRAIL-induced apoptosis of melanoma. Cancer Res 1999; 59:2747 – 53.

24. Komarov PG, Komarova EA, Kondratov RV, et al. A chemical inhibitor of p53 that protects mice from the side effects of cancer therapy. Science 1999;285:1733 – 7.

25. Li R, Moudgil T, Ross HJ, Hu HM. Apoptosis of non-small-cell lung cancer cell lines after paclitaxel treatment involves the BH3-only proapoptotic protein Bim. Cell Death Differ 2005;12:292 – 303.

26. Zha J, Harada H, Yang E, Jockel J, Korsmeyer SJ. Serine phosphorylation of death agonist BAD in response to survival factor results in binding to 14-3-3 not Bcl-X. Cell 1996;87:619 – 28.

27. Georgoulias V. Doectaxel (Taxotere) in the treatment of non-small cell lung cancer. Curr Med Chem 2002;9:869 – 77.

28. Johnson DE, Gastman BR, Wieckowski E, et al. Inhibitor of apoptosis protein hILP undergoes caspase-mediated cleavage during T lymphocyte apoptosis. Cancer Res 2000;60:1818 – 23.

29. Lassus P, Optiz-Araya X, Lazebnik Y. Requirement for caspase-2 in stress-induced apoptosis before mitochondrial permeabilization. Science 2002;297:1352 – 4.

30. Robertson JD, Enoksson M, Suomela M, Zhivotovsky B, Orrenius S. Caspase-2 acts upstream of mitochondria to promote cytochrome *c* release during etoposide-induced apoptosis. J Biol Chem 2002;277: 29803 – 9.

31. Guo Y, Srinivasula SM, Druilhe A, Fernandes-Alnemri T, Alnemri ES. Caspase-2 induces apoptosis by releasing proapoptotic proteins from mitochondria. J Biol Chem 2002;277:13430 – 7.

32. Nihal M, Ahmad N, Mukhtar H, Wood GS. Anti-proliferative and proapoptotic effects of (−)-epigallocatechin-3-gallate on human melanoma: possible implications for the chemoprevention of melanoma. Int J Cancer 2005;114:513 – 21.

33. Hsu YT, Youle RT. Bax in murine thymus is soluble monomeric protein that displays differential detergent-induced conformations. J Biol Chem 1998;273:10777 – 83.

34. Griffiths GJ, Dubrez L, Morgan CP, et al. Cell damage-induced conformational changes of the pro-apoptotic protein Bak *in vivo* precede the onset of apoptosis. J Cell Biol 1999;144:903 – 14.

35. Dewson G, Snowden RT, Almond JB, Dyer MJ, Cohen GM. Conformational changes and mitochondrial translocation of Bax accompany proteasome inhibitor-induced apoptosis of chronic lymphocytic leukemia cells. Oncogene 2003;22:2643 – 54.

36. Tinel A, Tschopp J. The PIDDosome, a protein complex implicated in activation of caspase-2 in response to genotoxic stress. Science 2004; 304:843 – 6.

37. Harvey NL, Butt AJ, Kumar S. Functional activation of Nedd2/ICH-1 (caspase-2) is an early process in apoptosis. J Biol Chem 1997;272: 13134 – 9.

38. Duan H, Dixit VM. RAIDD is a new ''death'' adaptor molecule. Nature 1997;385:86 – 9.

39. Ahmad M, Seinivasula SM, Wang L, et al. CRADD, a novel human apoptotic adaptor molecule for caspase-2, and FasL/tumor necrosis factor receptor-interacting protein RIP. Cancer Res 1997;57:615 – 9.

40. Lavrik IN, Golks A, Baumann S, Krammer PH. Caspase-2 is activated at the CD95 death-inducing signaling complex in the course of CD95-induced apoptosis. Blood 2006;108:559 – 65.

41. Paroni G, Henderson C, Schneider C, Brancolini C. Caspase-2 can trigger cytochrome *c* release and apoptosis from the nucleus. J Biol Chem 2002;277:15147 – 61.

42. Sawada M, Hayes P, Matsuyama S. Cytoprotective membrane-permeable peptides designed from Bax-binding domain of Ku70. Nat Cell Biol 2003;5:352 – 7.

43. Guo B, Zhai D, Cabezas E, et al. Human peptide suppresses apoptosis by interfering with Bax activation. Nature 2003;423:456 – 61.

44. Zhang XD, Wu JJ, Gillespie SK, Borrow JM, Hersey P. Human melanoma cells selected for resistance to apoptosis by prolonged exposure to TRAIL are more vulnerable to necrotic cell death induced by Cisplatin. Clin Cancer Res 2006;12:1355 – 64.